OXFORD UNIVERSITY PRESS | Schizophrenia Bulletin

Dysconnectivity in schizophrenia revisited: abnormal temporal organization of dynamic functional connectivity in patients with a first episode of psychosis

Journal:	*Schizophrenia Bulletin*
Manuscript ID	SZBLTN-ART-21-0800.R3
Manuscript Type:	Regular Article
Date Submitted by the Author:	11-Oct-2022
Complete List of Authors:	Ramirez-Mahaluf, Juan ; Pontificia Universidad Católica de Chile, Psychiatry Tepper, Ángeles; Pontificia Universidad Catolica de Chile, Psychiatry Alliende, Luz; Pontificia Universidad Católica de Chile, Psychiatry Carlos Mena, Carlos ; Pontificia Universidad Católica de Chile, Psychiatry; University College London, Institute of Cognitive Neuroscience Castañeda, Carmen; Instituto Psiquiátrico Dr. José Horwitz Barak, Programa de Intervención Temprana Iruretagoyena, Barbara; Instituto Psiquiátrico Dr. José Horwitz Barak, Programa de Intervención Temprana Nachar, Ruben; Instituto Psiquiátrico Dr. José Horwitz Barak Reyes-Madrigal, Francisco ; Instituto Nacional de Neurologia y Neurocirugia, Laboratory of Experimental Psychiatry León-Ortiz, Pablo; Instituto Nacional de Neurologia y Neurocirugia, Laboratory of Experimental Psychiatry Mora-Durán, Ricardo; Hospital Psiquiátrico Fray Bernardino Álvarez, Emergency Ossandón, Tomás; Pontificia Universidad Católica de Chile, Psychiatry; Pontificia Universidad Católica de Chile, Center for Integrative Neuroscience González-Valderrama, Alfonso; Instituto Psiquiátrico Dr J Horwitz Barak, Early Intervention Program; Universidad Finis Terrae, School of Medicine Undurraga, Juan; Instituto Psiquiátrico Dr. José Horwitz Barak, ; Clinica Alemana Universidad del Desarrollo, Neurology and Psychiatry de la Fuente-Sandoval, Camilo; Instituto Nacional de Neurologia y Neurocirugia, Laboratory of Experimental Psychiatry; Instituto Nacional de Neurologia y Neurocirugia, Neuropsychiatry Department Crossley, Nicolas; Pontificia Universidad Católica de Chile, Psychiatry; Pontificia Universidad Católica de Chile, Biomedical Imaging Center; Millennium Nucleus for Cardiovascular Magnetic Resonance; King's College London, Institute of Psychiatry, Psychology and Neuroscience
Keywords:	meta-states, dynamic connectivity, antipsychotics, schizophrenia, brain networks, graph analysis

Dysconnectivity in schizophrenia revisited: abnormal temporal organization of dynamic functional connectivity in patients with a first episode of psychosis

Juan P. Ramirez-Mahaluf[1], Ángeles Tepper[1], Luz Maria Alliende[1], Carlos Mena[1,2], Carmen Paz Castañeda[3], Barbara Iruretagoyena[3], Ruben Nachar[3], Francisco Reyes-Madrigal[4], Pablo León-Ortiz[4], Ricardo Mora-Durán[5], Tomas Ossandon[1,6], Alfonso Gonzalez-Valderrama[3,7], Juan Undurraga[3,8], Camilo de la Fuente-Sandoval[4,9, †], Nicolas A. Crossley[1 ,10, 11, 12, †]

[†]**These authors contributed equally to this work.**

Author affiliations:

1 Department of Psychiatry, School of Medicine, Pontificia Universidad Católica de Chile, Santiago, Chile.

2 Institute of Cognitive Neuroscience, University College London, London, UK.

3 Early Intervention Program, Instituto Psiquiátrico Dr. J Horwitz Barak, Santiago, Chile.

4 Laboratory of Experimental Psychiatry, Instituto Nacional de Neurología y Neurocirugía, Mexico City, Mexico

5 Emergency Department, Hospital Fray Bernardino Álvarez, Mexico City, Mexico

6 Center for Integrative Neuroscience, School of Medicine, Pontificia Universidad Católica de Chile, Santiago, Chile.

7 School of Medicine, Universidad Finis Terrae, Chile.

8 Department of Neurology and Psychiatry, Faculty of Medicine, Clínica Alemana Universidad del Desarrollo, Chile.

9 Neuropsychiatry Department, Instituto Nacional de Neurología y Neurocirugía, Mexico City, Mexico

10 Biomedical Imaging Center, Pontificia Universidad Católica de Chile.

11 Millennium Nucleus for Cardiovascular Magnetic Resonance, Chile.

12 Institute of Psychiatry, Psychology and Neuroscience, King's College London, London UK.

Corresponding author:

Nicolas Crossley

Diagonal Paraguay 362, Santiago, Chile

ncrossley@uc.cl

or

Camilo de la Fuente-Sandoval

Av. Insurgentes Sur 3877, Mexico City, Mexico

fcamilo@unam.mx

Running title: Dysconnectivity revisited

Abstract: 250

Text (excluding abstract and references): 3,999

Abstract

Background and Hypothesis: Abnormal functional connectivity between brain regions is a consistent finding in schizophrenia, including functional MRI studies. Recent studies have highlighted that connectivity changes in time in healthy subjects. We here examined the temporal changes in functional connectivity in patients with a first-episode of psychosis (FEP). Specifically, we analyzed the temporal order in which whole-brain organization states were visited.

Study Design: Two case-control studies, including in each sample a subgroup scanned a second time after treatment. Chilean sample included 79 patients with a FEP and 83 healthy controls. Mexican sample included 21 antipsychotic-naïve FEP patients and 15 healthy controls. Characteristics of the temporal trajectories between whole-brain functional connectivity meta-states were examined via resting-state functional MRI using elements of network science. We compared the cohorts of cases and controls and explored their differences as well as potential associations with symptoms, cognition and antipsychotic medication doses.

Study Results: We found that the temporal sequence in which patients' brain dynamics visited the different states was more redundant and segregated. Patients were less flexible than controls in changing their network in time from different configurations, and explored the whole landscape of possible states in a less efficient way. These changes were related to the dose of antipsychotic the patients were receiving. We replicated the relationship with antipsychotic medication in the antipsychotic-naïve FEP sample scanned before and after treatment.

Conclusions: We conclude that psychosis is related to a temporal disorganization of the brain's dynamic functional connectivity, and this is associated with antipsychotic medication use.

Keywords: dynamic connectivity, meta-states, antipsychotic, schizophrenia, brain networks, graph analysis.

Introduction

The dysconnectivity hypothesis of schizophrenia proposes that this disorder is due to an abnormal interaction between distant brain regions, rather than a single localized brain dysfunction[1,2]. Neuroimaging studies have provided evidence supporting this idea, showing abnormal structural[3] and functional connectivity in several networks[4] in patients.

More recently, functional MRI studies have shown that the brain's slow oscillatory activity and interactions between regions in health are not static, but rather change over time[5–7]. This evolving activity goes through periods of stable dynamics with a particular whole-brain organization or meta-states[8–10]. Opening the temporal domain of brain functional connectivity poses several questions to the dysconnectivity hypothesis of schizophrenia. Studies have shown that machine-learning algorithms are better at identifying schizophrenia from other disorders when the time-varying connectivity data is included, rather than the average or static connectivity matrices[11–13]. This suggests that temporal dynamics have valuable information about schizophrenia's pathophysiology.

Studies have focused on understanding how specifically is the dynamic functional connectivity abnormal in schizophrenia. We could divide the existing approaches into three groups of studies (Figure 1A). The first group suggest that dysconnectivity in schizophrenia (localized or global) is a transient rather than a constant state, more prevalent during specific periods of brain activity[14–16]. The second group highlight that functional connectivity within these transient states might not be different in patients compared to controls. Instead, it is the amount of time that patients remain on certain whole-brain meta-states that differs, so when examining "static" (average) functional connectivity differences between groups emerge[17–20]. The third group emphasize the sequential (temporal) nature of these dynamics, which was not necessarily addressed in the two other groups. Rather than focusing on the characteristics of the individual states (group 1) or their number (group 2), they examine the time domain and the changes between these states. They have done this by thinking of the dynamic functional network as linked or multiplex networks[21], with networks stacked according to the passing of time, or else by examining the nodal connections evolving in time[22] (Figure 1B). Unlike the two first groups, the characterization of these dynamic changes is not trivial to the order in which time passes.

The present study aims to contribute to our understanding of the temporal dynamics in the dysconnectivity state in schizophrenia by looking at a new aspect in the temporal transitions in brain activity, which is related to the third group of studies described above. For each time period (time window), we examined the whole-brain interactions or brain states, which happen to repeat themselves in time[9,10]. Just as one can build different words and sentences with the same letters by organizing them in alternative order (Figure 1C), we recently showed that the sequence in which the brain explores these brain states in healthy subjects is not random, and is related to general cognition and motor abilities[23]. Some healthy subjects tend to revisit meta-states forming a redundant trajectory, or visit consecutive meta-states that are similar, characteristics that were associated with lower general cognition. We here used this same approach based on network science to study the transitions between brain meta-states from functional MRI data of individuals experiencing a first-episode of psychosis (FEP) and healthy controls. Based on their relationship with cognition in healthy controls, we examined two main questions:

1) do patients tend to revisit whole-brain configuration meta-states shortly after leaving them, providing a more redundant trajectory than healthy controls?

2) are patients able to consecutively switch from very different brain meta-states and visit all the existing states efficiently?

We were also interested in the clinical characteristics associated with any observed differences in the dynamic changes between whole-brain meta-states. In particular, we explored its relationship with cognition, symptoms severity, and the use of antipsychotics, which are known to disrupt brain connectivity[24]. We hypothesized that patients with FEP would present a more redundant dynamic path when visiting different meta-states and a less efficient overall trajectory, when compared to healthy controls. This could be associated with difficulties in cognition and the use of antipsychotic medication. We addressed these questions in two first-episode samples and their matched healthy controls, exploring the replicability of our findings. Furthermore, we included repeated measurement of our subjects, which for one sample included before and after antipsychotic treatment.

Materials and methods

Subjects:

Our analyses included two datasets of resting-state fMRI data. The first included 79 patients admitted with a FEP to the early intervention program ward from the Instituto Psiquiátrico José Horwitz in Santiago, Chile[25]. Patients fulfilled criteria for a psychotic episode according to the Mini-International Neuropsychiatric Interview (MINI)[26]. Twelve patients presented an affective psychosis. Patients did not present any neurological, medical illness, comorbidity with other psychiatric disorders, and psychomotor agitation. The inclusion and exclusion criteria were evaluated by their treating psychiatrists and through standardized evaluations at the scanning time. A history of substance use was not considered as an exclusion criterion, but cases with substance-induced psychosis were excluded. Patients were scanned at the earliest possible opportunity. On average, they were treated with antipsychotics for 24.6 ± 13.1 days (mean ± standard deviation) before the baseline scan. A subgroup of 27 patients were rescanned after an average of 111.6 ± 37.7 days. Eighty-three healthy participants without a lifetime history of psychotic disorder, no first-degree family history of psychotic disorders, and no current history of any mental disorder were also included, scanning them at baseline. Thirty-two healthy controls were reassessed at 128.3 ± 47.7 (mean ± standard deviation) days. The study was approved by the Ethics Committee of the Pontificia Universidad Católica de Chile (Ref: 15-297) and Servicio de Salud Metropolitano Norte. Written informed consent was obtained from all participants.

The second cohort included 21 patients with non-affective FEP and 15 healthy participants from the Instituto Nacional de Neurología y Neurocirugía, Mexico. The Structured Clinical Interview for DSM-5 was utilized to determine inclusion. Patients were antipsychotic-naïve at baseline. Exclusion criteria included a concomitant medical or neurological illness, current substance abuse or history of substance dependence (excluding nicotine), comorbidity with other psychiatric disorders, a high risk for suicide, and psychomotor agitation. Fifteen age- and sex-matched healthy controls were also enrolled and assessed in the same manner as the patients. Controls with a history of psychiatric illness or a family history of psychosis were excluded. Fifteen patients were re-scanned and re-assessed at 4-week follow-up, alongside

twelve healthy controls. The study was approved by the Ethics Committee of the Instituto Nacional de Neurología y Neurocirugía, and written informed consent was obtained from all participants.

Table 1 provides further demographic and clinical information about these two samples and supplementary table 1 provides information about the antipsychotic medication. All patients from Mexico were treated with risperidone at the follow-up.

Both samples were assessed clinically in both time points using symptom rating scales (PANSS)[27] and a neuropsychological assessment (MATRICS Consensus Cognitive Battery)[28,29]. Doses of antipsychotics were converted to chlorpromazine equivalents using the DDD method[30].

Data acquisition and pre-processing:

Our first sample was scanned in a Philips Ingenia 3-T MRI with a 16-channel coil. Resting-state images were acquired for 8.33 minutes (195 volumes), while participants had their eyes open, using an EPI acquisition with a TR of 2.5s, TE 32ms, and a flip angle of 82°. Forty slices with a continuous descending order were acquired, using a field of view of 220x220mm, and an isotropic voxel size of 2.75mm. A structural T1-weighted image with a voxel size of $1.0mm^3$ isotropic, a minimum TI delay of 965.2, TE=3.5, TR=7.7 and flip angle of 8° was also acquired.

The second sample were scanned in a 3-T Siemens Skyra scanner with a 20-channel radio frequency coil. Resting-state images were acquired during 5.06 minutes (645 multiband volumes) while participants kept their eyes opened. T2*-weighted functional images were acquired using a gradient-echo EPI sequence with TE=29ms, TR=0.46s, flip angle=44°, slice thickness=3mm, slice gap=3mm, field of view 268mm, base resolution=82, multiband acceleration factor=8, voxel size=3.3mm×3.3mm×3.0mm. A structural T1-weighted image with a voxel size of $1.0mm^3$ isotropic, a minimum TI delay of 965.2, TE 3.5, TR 2.3 and flip angle of 9° was also acquired.

Preprocessing of the functional images of both datasets followed a previously published pipeline[31]. Briefly, this included slice-time correction, realignment, normalization, spatial smoothing with a 6mm FWHM kernel and temporal filtering between 0.008 and 0.08 Hz. Management of residual movement was performed using an automated-ICA method[32].

Data analysis:

Identification of temporal meta-states

Our analyses first involved identifying the set of whole-brain configurations or meta-states that the functional brain dynamics visited over time. We first divided the brain into similarly-sized regions using a previously established template (638 nodes)[33], and used multiplication of temporal derivatives to measure the functional connectivity between all pairs of regions in non-overlapping temporal windows. Multiplication of temporal derivatives[34] has shown high sensitivity to changes in functional connectivity and robustness to noise introduced by head movement, making it appropriate for dynamic functional connectivity analysis. Based on our previous study examining temporal dynamics at relatively short windows with sparse sampling[23], we used time windows of length of 2 volumes (5040ms) for the Chilean cohort and 3 volumes (1380ms) for the Mexican cohort. We therefore obtained a 638 x N time windows for each subject.

The similarity between the functional connectivity organization of each subjects' time windows was then clustered using k-means[35]. This process assigned each window to a specific meta-state. For example, starting with the original 97 windows in the Chilean sample, our clustering procedure grouped them into a reduced number of discrete states that the subject could repeatedly visit. Considering that there is no certainty about the number of discrete states that brain dynamics may explore, we analyzed a wide range of clusters (35-55).

Finally, we represented the temporal trajectories between visited brain states as a directed graph. Here each meta-state was represented as a node and the transitions between meta-states as directed edges. A weight was assigned to each edge according to the number of times the brain transitioned between a pair of meta-states, in the direction of the edge. Supplementary figure 1 summarizes the construction of this directed and weighted network.

Network parameters examined

We explored differences in temporal trajectories between groups using the following metrics on the weighted-directed graphs:

Measures of redundancy in the temporal paths

a) modularity of the graph[36], which examines how easy it is to divide a specific network into highly connected subgroups or modules. Considering that the strength of the connections is based on the amount of time the brain transits through those states, a highly modular network would indicate a temporal trajectory characterized by a high likelihood to revisit certain groups of states.

b) local efficiency of the network[37], a measure closely related to the clustering of a network, describing the level of connectivity between neighbors of a node.

Measures exploring transitions between different brain states

a) transition cost[23], a global parameter defined as the distance between one meta-state and the next one (1 – correlation coefficient of their connectivity matrices). Transitions between consecutive states that are very different in their connectivity patterns (low correlation) would have a high cost. This could reflect a higher metabolic cost associated with switching from one connectivity pattern to another.

We also analyzed two different aspects related to this cost measure: the immobility of the network (number of times the brain dynamics remained in the same meta-state between two consecutive windows) and the leap size (the transition cost without considering immobility periods).

b) global efficiency[37], a global measure based on the shortest paths between states. It provides an indicator of how easy it is, on average, for the brain to transition from one state to any other.

Low global efficiency could be due to a higher average transition costs or an inefficient organization of the connecting paths. We therefore measured the global efficiency of the transition network accounting for transition costs, or its cost-efficiency[38].

All these metrics are measured on directed graphs. Directed graph are relevant for path-length based metrics such as global, local efficiency and cost-efficiency. This is because nodes could be connected in one direction but not in opposite direction, unlike undirected graphs, where if two nodes are connected, this is for both directions (Supplementary figure 2).

For each measure, we calculated the area under the curve for the entire range of number of clusters used in the k-clustering algorithm of the meta-states. We then used this value for the linear mixed-effect model (described below).

Clinical analyses:

Both samples included repeated measurement data for some (but not all) participants. We therefore used a linear mixed-effect model, which provided the greatest power and flexibility as it allowed us to inform our model from all the available measurements. We first looked at differences between patients and controls, using the following model:

Graph metric ~ age + gender + framewise-displacement + case + (1|subject) (1)

Subject variable was defined as a random effect to account for repeated measures. Gender, age and a measure of within-scanner movement (framewise displacement[39]), were included as covariates of no interest.

Another mixed-effect model was constructed to explore the clinical importance of potential differences in these metrics. These included only patients, using the following model:

Graph metric ~ age + gender + framewise-displacement + PANSSp + PANSSn + MATRICS + Antipsychotic + (1|subject) (2)

We also included in the model above the variable affective for the Chile sample.

Supplementary Tables 2 and 3 provides demographic and clinical data organized according to the presence (or not) of repeated measurements.

Although our analysis did not explicitly examine changes before and after treatment (for which we had less data), by including the PANSS, cognitive functioning and antipsychotic medication in the mixed-effect analysis, our analyses could inform changes in time related to these variables. Analyses looking at changes before and after treatment in the participants with complete follow-up data are reported in the Supplementary Figures 3 and 4 and Supplementary Table 4 and 5.

Multiple comparisons were managed using false discovery rates for each of these analyses. For example, the analyses of the clinical features included 7 graph metrics and 4 variables of interest (28 comparisons). All data analyses were done with MATLAB (MathWorks, Natick, USA).

Data availability

All analyzes were performed using in-house Matlab scripts; this code is available from the authors upon request. Data is available from the authors upon request.

Results

We first present the result from our larger Chile sample, and then the replication sample Mexico.

Patients present redundant and segregated temporal dynamics

Previously, we showed that transition networks in the healthy brain could be decomposed into clusters of nodes with high connectivity between themselves[23]. This meant that brain dynamics evolved with periods visiting a specific group of global state configurations, eventually moving on to another set. Q values from Newman modularity algorithm were significantly higher for patients than controls, suggesting a more segregated network ($F_{1,216}$=8.67, P_{FDR}=0.013, Fig. 2A, Supplementary Table S6).

We then examined whether dynamic trajectories in patients were more redundant, frequently returning to recently visited meta-states, measuring the local efficiency. Patients' transition networks had significantly higher local efficiency ($F_{1,216}$=5.12, P_{FDR}=0.029, Fig. 2B, Supplementary Table S6) than healthy controls, showing a higher redundancy.

Less efficient trajectories in patients with psychosis

The global efficiency of transition networks describes how long brain dynamics traverse on average to get from one state to another. This metric was lower for patients ($F_{1,216}$=9.3, P_{FDR}=0.013), reflecting less efficient trajectories between brain states. Since edges of the network refer to time periods (changes between consecutive time windows), this could be interpreted as patients being slower to visit on average different meta-states compared to healthy subjects (Fig. 2C, Supplementary Table S6).

We then analyzed the costs of transitions, which we conceptualized as how much the brain had to change its connectivity pattern between one meta-state and the following one[23]. The transition cost was significantly lower in patients than in controls ($F_{1,216}$=6.45, P_{FDR}=0.021,

Fig. 2D, Supplementary Table S6). Further examination of the lower costs found in patients, we found that leap size was significantly lower compared controls ($F_{1,216}$=5.36, P_{FDR}=0.029, Fig. 2E, Supplementary Table S6). Additionally, immobility was significantly higher in patients ($F_{1,216}$=4.52, P_{FDR}=0.035, Fig. 2F, Supplementary Table S6). Thus, lower transition costs in patients were driven by dynamics that remained in the same meta-state more frequently and had a reduced capacity to move between very different meta-states.

Cost-efficiency (global efficiency normalized by the cost) in patients' network was also lower than in controls' ($F_{1,216}$=7.6, P_{FDR}=0.015, Fig. 2G, Supplementary Table S6).

Figure 2H-I illustrate these dynamic differences in a representative healthy control (Fig. 2H) and patient (Fig. 2I).

Associations between abnormal dynamic and clinical characteristics

Higher antipsychotic doses in patients were associated with more segregated and redundant trajectories. We found a positive association between dose of antipsychotics and modularity (Q value) of the transition network (*segregation*; $F_{1,97}$=11.58, P_{FDR}=0.021, Fig. 3A, Supplementary Table S7), as well as a with its local efficiency (*redundancy*; $F_{1,97}$=7.5, P_{FDR}=0.041, Fig. 3B, Supplementary Table S7).

Antipsychotic doses were associated with changes in the path length-based measures, including a negative association between dose and global efficiency ($F_{1,97}$=10.73, P_{FDR}=0.021, Fig. 3C, Supplementary Table S7). We also found a negative association between the cost-efficiency of the transition networks and doses ($F_{1,97}$=8.66, P_{FDR}=0.038, Fig. 3D, Supplementary Table S7).

There was a negative association between negative symptoms and leap size ($F_{1,97}$=8.08, P_{FDR}=0.038), with lower negative symptoms associated with a higher capacity to transit between remarkably different brain states (Fig. 3E, Supplementary Table S7).

There were no significant associations between dynamic functional network and cognitive measures.

Transition networks in antipsychotic-naïve patients with first episode psychosis

We then explored case-control differences using a second dataset of resting-state fMRI of 21 antipsychotics-naïve patients with FEP (Mexico dataset). 15 patients were re-scanned one month later after receiving treatment. Patients were similar in demographics as shown in Table 1. The scanning sequence used was different from the first cohort, with a higher temporal resolution, and a smaller temporal window size used. However, as figure S5 shows, healthy controls from this sample displayed a similar non-trivial temporal organization in their brain dynamics to the sample from Chile and the Human Connectome Project[23]. It also displayed similar within-subject reliability in metrics such as leap size (Figure S6 and Supplementary table S8)[23].

We did not find any significant differences in the configuration of transition networks between patients and controls (Supplementary Fig. S7 and Supplementary Table S9). However, exploring clinical features we found a positive association between local efficiency and doses of antipsychotics ($F_{1,28}$=4.31, P_{unc}=0.047, Fig. 4A, Supplementary Table S10) and a trend negative association between global efficiency and doses of antipsychotics ($F_{1,28}$=3.996, P_{unc}=0.055, Fig. 4B, Supplementary Table S10), partially replicating the main results of the Chilean dataset. In addition, exploring changes before and after treatment in the patients with complete follow-up data, we found that after treatment modularity (Q) was significantly higher (P_{unc}=0.0347, Supplementary Fig. 4A, Supplementary Table S5) and global efficiency was significantly lower (P_{unc}=0.0182, Supplementary Fig. 4B, Supplementary Table S5).

Discussion

By using a novel method that focuses on the order in which certain brain configurations are visited over time, we here contribute further to our understanding of dysconnectivity in schizophrenia in the temporal domain. We found that patients with psychosis present a higher redundancy and segregation in their temporal trajectories than controls. We also found that patients are less efficient in visiting different brain states in time. These changes were associated with the antipsychotic dose received, possibly through dopaminergic blockage. Finally, the association between redundant and inefficient trajectories and antipsychotic doses

was replicated on a smaller sample of antipsychotic naïve patients treated during one month with lower doses of antipsychotics.

Patients presented differences in several functional dynamic metrics. These results add up to previous findings showing that patients present differences in the transition probability between brain states and in the amount of time they remain in several brain states relative to controls[15,17,18]. Together, they suggest that the dysconnectivity hypothesis should be further expanded to consider this abnormal evolving activity, a state of temporal dis-organization. In other words, schizophrenia might not only be linked to problems in the building blocks of the brain's interacting activity, but also in the way they are sequentially visited. The latter would be akin to creating aberrant sentences with normal words by organizing them in a nonsensical sequence.

How do we interpret our findings? One can see a global common picture emerging of a slowed-down system, which probably has difficulties in varying its dynamic repertoire, and tends to repeat itself. That is how we found an increase in modularity and local efficiency in the trajectories, which increases the redundancy in the dynamics; a decrease in its cost, which makes it less able to switch plastically to different states; and a lower global efficiency, which describes a landscape of possible dynamics which is visited in a slower way. Such an interpretation complements the traditional implications of the dysconnectivity hypothesis. The temporal dysconnectivity view might give a fuller picture to a complex clinical presentation, providing possible explanations for things such as processing speed difficulties[40], the tendency to perseverate[41] or catatonic repetition[42]. However intuitive, some aspects of the data do not fully support this explanation, particularly the lack of associations between dynamics and global cognition in patients.

One of the strengths of our study is the inclusion of a second sample which replicated some of our results, namely those related to antipsychotic medication. The replication sample was small, and therefore was under-powered to find medium or small effects, such as those possibly related to being a case. Patients received low-dose antipsychotic medication for a month only, making it even more interesting to see that a replication with antipsychotic dose and local efficiency was found. These associations with antipsychotic doses must be interpreted carefully, since the dopamine-blocking ability differs between the different antipsychotic medications used, and conversion to common standards (chlorpromazine equivalent) might not necessarily eliminate all this variation. Functional connectivity changes observed after

antipsychotic initiation have been associated with symptomatic improvement and described as a normalization of the connectivity[43,44]. However, disruptions in the functional network organization in healthy subjects have also been reported after pharmacologically-induced decreased dopaminergic tone[45,46]. Our replicated findings showing that antipsychotics are associated with a disrupted temporal organization do not necessarily contradict the proposed localized normalization of connectivity also associated with them, as our method examines brain properties that are not seen by usual "static" analyses. We previously found a significant association between cognition and temporal dynamics in healthy subjects[23], which we did not replicate within patients in this study. Nevertheless, one could hypothesize that the antipsychotics' limited effect on cognition[47], and possibly its deleterious effect at high doses, might be related to their lack of beneficial effect on temporal dynamics.

From a dynamic point of view, the relationship between antipsychotic use and network dynamics has been described using attractor-based computational frameworks[48,49]. Acute psychosis, particularly high positive symptoms, has been associated with unstable attractors in brain activity. On the contrary, D2 antagonists would lead to more stable states. Our results support these predictions[49], suggesting that dopamine modulation generates an over-stability of meta-states resulting in slower transitions between them, with more redundant trajectories and difficulties switching to novel (different) states.

The main limitation of this study is the small sample size of antipsychotic-naïve patients in our replication sample. In addition, patients were recruited in tertiary centers, which could bias the sample towards more severe cases usually treated with higher doses of antipsychotics, and limit the generalizability of the results. The samples also differed in the inclusion of patients with affective psychosis, symptoms severity, and age. Although these limitations were addressed by incorporating these variables in the mixed-effect models, the lack of homogeneity between samples must be taken into account when interpreting the results.

In conclusion, by using a novel method focusing on the temporal changes of the brain's functional configurations, we found that FEP patients presented a temporal disorganization in their brain dynamics. Namely, their trajectories were more redundant, presented higher segregation, and visited consecutively more similar brain states than healthy controls. In addition, we found that these changes were associated with antipsychotic use.

Funding

This work was funded by the Agencia Nacional de Investigación y Desarrollo from Chile (ANID), through its programs ANILLO PIA ACT1414 and PIA ACT192064, FONDECYT postdoctorado (Ref: 3190311 to Juan P. Ramirez-Mahaluf), and FONDECYT regular (Ref: 1200601 to Nicolas A.Crossley, Ref: 1180932 to Tomas Ossandon, Ref: 1180358 to Juan Undurraga). Nicolas A. Crossley is supported by the Millennium Science Initiative of ANID Chile, grant Nucleus for Cardiovascular Magnetic Resonance. Pablo León-Ortiz, Francisco Reyes-Madrigal and Camilo de la Fuente-Sandoval are supported by Consejo Nacional de Ciencia y Tecnología / Sistema Nacional de Investigadores, Mexico, and National Institutes of Health grant R01 MH110270 to Camilo de la Fuente-Sandoval.

Competing interests

Drs Reyes-Madrigal, León-Ortiz and Mora-Durán have received speaking fees from Janssen (Johnson & Johnson). Dr. Crossley has received personal fees from Janssen outside the submitted work. All other authors reported no competing interests.

Supplementary material

Supplementary material is available at *Schizophrenia Bulletin* online.

References

1. Friston KJ, Frith CD. Schizophrenia: a disconnection syndrome? *Clin Neurosci*. 1995;3(2).
2. Pettersson-Yeo W, Allen P, Benetti S, McGuire P, Mechelli A. Dysconnectivity in schizophrenia: Where are we now? *Neurosci Biobehav Rev*. 2011;35(5):1110-1124. doi:10.1016/j.neubiorev.2010.11.004
3. Wheeler AL, Voineskos AN. A review of structural neuroimaging in schizophrenia: From connectivity to connectomics. *Front Hum Neurosci*. 2014;8(AUG). doi:10.3389/fnhum.2014.00653
4. Calhoun VD, Eichele T, Pearlson G. Functional brain networks in schizophrenia: A

review. *Front Hum Neurosci*. 2009;3(AUG). doi:10.3389/neuro.09.017.2009

5. Chang C, Glover GH. Time-frequency dynamics of resting-state brain connectivity measured with fMRI. *Neuroimage*. 2010;50(1):81-98. doi:10.1016/j.neuroimage.2009.12.011
6. Hutchison RM, Womelsdorf T, Allen EA, et al. Dynamic functional connectivity: Promise, issues, and interpretations. *Neuroimage*. 2013;80:360-378. doi:10.1016/j.neuroimage.2013.05.079
7. Smith SM, Miller KL, Moeller S, et al. Temporally-independent functional modes of spontaneous brain activity. *Proc Natl Acad Sci U S A*. 2012;109(8):3131-3136. doi:10.1073/pnas.1121329109
8. Betzel RF, Fukushima M, He Y, Zuo XN, Sporns O. Dynamic fluctuations coincide with periods of high and low modularity in resting-state functional brain networks. *Neuroimage*. 2016;127:287-297. doi:10.1016/j.neuroimage.2015.12.001
9. Shine JM, Koyejo O, Poldrack RA. Temporal metastates are associated with differential patterns of time-resolved connectivity, network topology, and attention. *Proc Natl Acad Sci*. 2016;113(35):9888-9891. doi:10.1073/pnas.1604898113
10. Vidaurre D, Smith SM, Woolrich MW. Brain network dynamics are hierarchically organized in time. *Proc Natl Acad Sci*. 2017:201705120. doi:10.1073/pnas.1705120114
11. Rabany L, Brocke S, Calhoun VD, et al. Dynamic functional connectivity in schizophrenia and autism spectrum disorder: Convergence, divergence and classification. *NeuroImage Clin*. 2019;24. doi:10.1016/j.nicl.2019.101966
12. Rashid B, Arbabshirani MR, Damaraju E, et al. Classification of schizophrenia and bipolar patients using static and dynamic resting-state fMRI brain connectivity. *Neuroimage*. 2016;134:645-657. doi:10.1016/j.neuroimage.2016.04.051
13. Du Y, Hao H, Wang S, Pearlson GD, Calhoun VD. Identifying commonality and specificity across psychosis sub-groups via classification based on features from dynamic connectivity analysis. *NeuroImage Clin*. 2020;27. doi:10.1016/j.nicl.2020.102284
14. Li C, Dong M, Womer FY, et al. Transdiagnostic time-varying dysconnectivity across major psychiatric disorders. *Hum Brain Mapp*. 2021;42(4):1182-1196. doi:10.1002/hbm.25285
15. Mennigen E, Fryer SL, Rashid B, et al. Transient Patterns of Functional Dysconnectivity in Clinical High Risk and Early Illness Schizophrenia Individuals Compared with Healthy Controls. *Brain Connect*. 2019;9(1):60-76. doi:10.1089/brain.2018.0579

16. Du Y, Fryer SL, Fu Z, et al. Dynamic functional connectivity impairments in early schizophrenia and clinical high-risk for psychosis. *Neuroimage*. 2018;180:632-645. doi:10.1016/j.neuroimage.2017.10.022

17. Du Y, Pearlson GD, Yu Q, et al. Interaction among subsystems within default mode network diminished in schizophrenia patients: A dynamic connectivity approach. *Schizophr Res*. 2016;170(1):55-65. doi:10.1016/j.schres.2015.11.021

18. Damaraju E, Allen EA, Belger A, et al. Dynamic functional connectivity analysis reveals transient states of dysconnectivity in schizophrenia. *NeuroImage Clin*. 2014;5:298-308. doi:10.1016/j.nicl.2014.07.003

19. Covington HE, Lobo MK, Maze I, et al. Antidepressant effect of optogenetic stimulation of the medial prefrontal cortex. 30(48):16082-16090. doi:10.1523/JNEUROSCI.1731-10.2010

20. Fu Z, Iraji A, Sui J, Calhoun VD. Whole-Brain Functional Network Connectivity Abnormalities in Affective and Non-Affective Early Phase Psychosis. *Front Neurosci*. 2021;15. doi:10.3389/fnins.2021.682110

21. Gifford G, Crossley N, Kempton MJ, et al. Resting state fMRI based multilayer network configuration in patients with schizophrenia. *NeuroImage Clin*. 2020;25. doi:10.1016/j.nicl.2020.102169

22. Sun Y, Collinson SL, Suckling J, Sim K. Dynamic reorganization of functional connectivity reveals abnormal temporal efficiency in schizophrenia. *Schizophr Bull*. 2019;45(3):659-669. doi:10.1093/schbul/sby077

23. Ramirez-Mahaluf JP, Medel V, Tepper Á, et al. Transitions between human functional brain networks reveal complex, cost-efficient and behaviorally-relevant temporal paths. *Neuroimage*. 2020;219:117027. doi:10.1016/j.neuroimage.2020.117027

24. Honey GD, Suckling J, Zelaya F, et al. Dopaminergic drug effects on physiological connectivity in a human cortico-striato-thalamic system. *Brain*. 2003;126(8):1767-1781. doi:10.1093/brain/awg184

25. González-Valderrama A, Castañeda CP, Mena C, et al. Duration of untreated psychosis and acute remission of negative symptoms in a South American first-episode psychosis cohort. *Early Interv Psychiatry*. 2017;11(1):77-82. doi:10.1111/eip.12266

26. Sheehan D V., Lecrubier Y, Sheehan KH, et al. The Mini-International Neuropsychiatric Interview (M.I.N.I.): The development and validation of a structured diagnostic psychiatric interview for DSM-IV and ICD-10. In: *Journal of Clinical Psychiatry*. Vol 59. ; 1998:22-33.

27. Kay SR, Fiszbein A, Opler LA. The positive and negative syndrome scale (PANSS) for schizophrenia. *Schizophr Bull*. 1987;13(2):261-276. doi:10.1093/schbul/13.2.261
28. Nuechterlein KH, Green MF, Kern RS, et al. The MATRICS consensus cognitive battery, part 1: Test selection, reliability, and validity. *Am J Psychiatry*. 2008;165(2):203-213. doi:10.1176/appi.ajp.2007.07010042
29. Kern RS, Nuechterlein KH, Green MF, et al. The MATRICS Consensus Cognitive Battery, part 2: Co-norming and standardization. *Am J Psychiatry*. 2008;165(2):214-220. doi:10.1176/appi.ajp.2007.07010043
30. Leucht S, Samara M, Heres S, Davis JM. Dose Equivalents for Antipsychotic Drugs: The DDD Method. *Schizophr Bull*. 2016;42:S90-S94. doi:10.1093/schbul/sbv167
31. Parkes L, Fulcher B, Yücel M, Fornito A. An evaluation of the efficacy, reliability, and sensitivity of motion correction strategies for resting-state functional MRI. *Neuroimage*. 2018;171:415-436. doi:10.1016/j.neuroimage.2017.12.073
32. Pruim RHR, Mennes M, van Rooij D, Llera A, Buitelaar JK, Beckmann CF. ICA-AROMA: A robust ICA-based strategy for removing motion artifacts from fMRI data. *Neuroimage*. 2015;112:267-277. doi:10.1016/j.neuroimage.2015.02.064
33. Crossley NA, Mechelli A, Vertes PE, et al. Cognitive relevance of the community structure of the human brain functional coactivation network. *Proc Natl Acad Sci*. 2013;110(28):11583-11588. doi:10.1073/pnas.1220826110
34. Shine JM, Koyejo O, Bell PT, Gorgolewski KJ, Gilat M, Poldrack RA. Estimation of dynamic functional connectivity using Multiplication of Temporal Derivatives. *Neuroimage*. 2015;122:399-407. doi:10.1016/j.neuroimage.2015.07.064
35. Peer M, Prüss H, Ben-Dayan I, Paul F, Arzy S, Finke C. Functional connectivity of large-scale brain networks in patients with anti-NMDA receptor encephalitis: an observational study. *The Lancet Psychiatry*. 2017;4(10):768-774. doi:10.1016/S2215-0366(17)30330-9
36. Newman MEJ. Modularity and community structure in networks. *Proc Natl Acad Sci*. 2006;103(23):8577-8582. doi:10.1073/PNAS.0601602103
37. Latora V, Marchiori M. Efficient behavior of small-world networks. *Phys Rev Lett*. 2001;87(19):198701-1-198701-198704. doi:10.1103/PhysRevLett.87.198701
38. Fornito A, Zalesky A, Bassett DS, et al. Genetic influences on cost-efficient organization of human cortical functional networks. *J Neurosci*. 2011;31(9):3261-3270. doi:10.1523/JNEUROSCI.4858-10.2011
39. Power JD, Mitra A, Laumann TO, Snyder AZ, Schlaggar BL, Petersen SE. Methods to

detect, characterize, and remove motion artifact in resting state fMRI. *Neuroimage*. 2014;84:320-341. doi:10.1016/j.neuroimage.2013.08.048

40. Dickinson D, Ramsey ME, Gold JM. Overlooking the obvious: A meta-analytic comparison of digit symbol coding tasks and other cognitive measures in schizophrenia. *Arch Gen Psychiatry*. 2007;64(5):532-542. doi:10.1001/archpsyc.64.5.532
41. Crider A. Perseveration in schizophrenia. *Schizophr Bull*. 1997;23(1):63-74. doi:10.1093/schbul/23.1.63
42. Fink M, Taylor MA. The catatonia syndrome: Forgotten but not gone. *Arch Gen Psychiatry*. 2009;66(11):1173-1177. doi:10.1001/archgenpsychiatry.2009.141
43. Kraguljac NV, White DM, Hadley N, et al. Aberrant hippocampal connectivity in unmedicated patients with schizophrenia and effects of antipsychotic medication: A longitudinal resting state functional mri study. *Schizophr Bull*. 2016;42(4):1046-1055. doi:10.1093/schbul/sbv228
44. Sarpal DK, Robinson DG, Lencz T, et al. Antipsychotic treatment and functional connectivity of the striatum in first-episode schizophrenia. *JAMA Psychiatry*. 2015;72(1):5-13. doi:10.1001/jamapsychiatry.2014.1734
45. Achard S, Bullmore E. Efficiency and cost of economical brain functional networks. *PLoS Comput Biol*. 2007;3(2):0174-0183. doi:10.1371/journal.pcbi.0030017
46. Carbonell F, Nagano-Saito A, Leyton M, et al. Dopamine precursor depletion impairs structure and efficiency of resting state brain functional networks. *Neuropharmacology*. 2014;84:90-100. doi:10.1016/j.neuropharm.2013.12.021
47. Baldez DP, Biazus TB, Rabelo-da-Ponte FD, et al. The effect of antipsychotics on the cognitive performance of individuals with psychotic disorders: Network meta-analyses of randomized controlled trials. *Neurosci Biobehav Rev*. 2021;126:265-275. doi:10.1016/j.neubiorev.2021.03.028
48. Loh M, Rolls ET, Deco G. A dynamical systems hypothesis of schizophrenia. *PLoS Comput Biol*. 2007;3(11):2255-2265. doi:10.1371/journal.pcbi.0030228
49. Rolls ET, Loh M, Deco G, Winterer G. Computational models of schizophrenia and dopamine modulation in the prefrontal cortex. *Nat Rev Neurosci*. 2008;9(9):696-709. doi:10.1038/nrn2462

Figure legends

Figure 1. State of the art.

An overview of dynamic functional connectivity studies in schizophrenia. (**A**) A summary of the existing approaches. Group 1 characterizes studies that focused on transient dysconnectivity state in schizophrenia. Group 2 represents literature that studied on the amount of time that patients remain on certain meta-states. Group 3 characterizes studies that examines characteristic of temporal dynamics, highlighting the temporal nature of dynamics. (**B**) In details, group 3 studies the dynamic functional network by examining the nodal connections evolving in time or multiplex networks. (**C**) Our approach differs from group 3 in that we study the dynamic functional connectivity by the construction of transition networks where each node is a meta-state and the links between nodes are the transitions between meta-states, and analyse the temporal order in meta-states were visited.

Figure 2. Topological and economical properties of transition networks and transition network examples of patients with first episode psychosis and healthy controls.

The plots show the residuals of the area under the curve for topological and economical properties in the transition graph for healthy controls (blue) and patients with first episode of psychosis (red). **A**, modularity (*Q* value). **B**, local efficiency. **C**, global efficiency. **D**, Transition cost. **E**, Leap size. **F**, Immobility. **G**, Cost-efficiency. The circles and error bar mark the mean and standard error of the mean.

The bottom figures shows transition networks from two subjects. Column **H** shows healthy control and column **I**, patient. The layout of the graph is such that the distance between nodes is proportional to their transition cost (1 – correlation of connectivity matrices). The color of the nodes denote the degree, the arrow of links represent the direction, and the width of links the number of transitions between the connected nodes (weight). Self-connections of the nodes represent consecutive periods (time windows) in which the brain remained in the same meta-state (i.e. immobility). The temporal path depicted in the transition graph of the healthy control spans longer distances (larger leap size), reaching other nodes rapidly (higher global efficiency), with apparently less redundant paths (lower local efficiency). In the transition

network of the patient the nodes are less connected, which implies going through more intermediate nodes to visiting meta-states (lower global efficiency).

Figure 3. Transition network properties are related to antipsychotic doses and negative symptoms.

Scatter plots **A-D** show significant associations between topological characteristics of the transition networks in patients and antipsychotic doses. **A**, modularity (*Q* value). **B**, local efficiency. **C**, global efficiency. **D**, Cost-efficiency. Scatter plot **E** show significant association between patient's leap size and negative symptoms. The error bar around the linear regression mark 95% CI.

Figure 4. Transition network properties are related to antipsychotic doses in the Mexican sample

Scatter plots showing the significant associations between topological characteristics of the transition networks in patients and antipsychotics doses. **A**, local efficiency. **B**, global efficiency. The error bar around the linear regression mark 95% CI.

Table 1. Demographical and clinical scales of Chilean and Mexican cohorts

	Chilean sample			Mexican sample		
	First-episode psychosis	**Healthy Control**	**p-Value**	**First-episode psychosis**	**Healthy Control**	**p-Value**
Demographical variables						
N Baseline (male)	79 (64)	83 (56)	0.074	21 (11)	15 (7)	0.735
N Follow up (male)	27 (20)	32 (19)	0.361	15 (8)	12 (6)	0.863
Age	20.2 ± 0.3	23.3 ±0.4	<0.001	27.3 ±1.2	24.2 ±0.6	0.094
Clinical scales and antipsychotic doses in patients						
	Baseline	***Follow-up***		***Baseline***	***Follow-up***	
PANSS total	69.3 ± 2.1	44 ± 3.1		110.3 ± 4.8	75.9 ± 7.5	
PANSS Positive symptoms	16.3 ± 0.7	9.4 ± 0.7		29.8 ± 1.2	17.3 ± 2.2	
PANSS Negative symptoms	20.4 ± 1	13 ± 1.5		26.6 ± 2.1	21.6 ± 2.9	
PANSS General symptoms	32.6 ± 0.9	21.6 ± 1.2		54 ± 2.4	37.1 ± 3.1	
MATRICS total score	29.9 ± 1.9	33.4 ± 3.1		24.6 ± 2.6	30.3 ± 2.8	
Antipsychotic doses (mg)*	537.5 ± 32.9	420.2 ± 50.1		0 ± 0	172 ± 17.4	

Antipsychotic doses expressed in chlorpromazine equivalents (Leucht et al. 2016). Mean ± SEM.

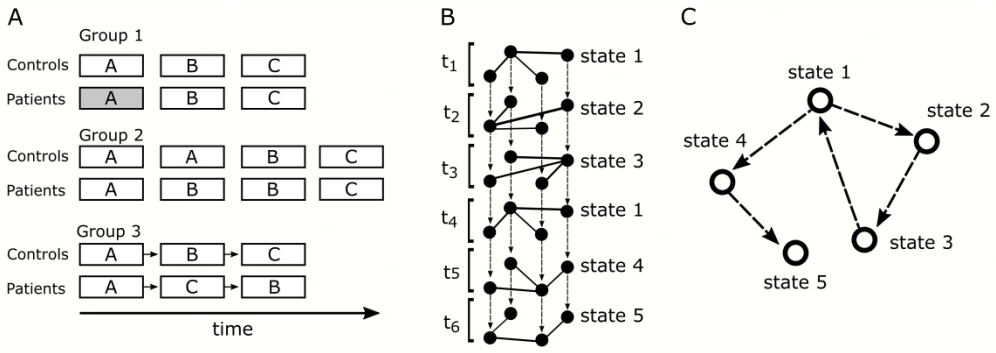

Figure 1. State of the art.
An overview of dynamic functional connectivity studies in schizophrenia. (A) A summary of the existing approaches. Group 1 characterizes studies that focused on transient dysconnectivity state in schizophrenia. Group 2 represents literature that studied on the amount of time that patients remain on certain meta-states. Group 3 characterizes studies that examines characteristic of temporal dynamics, highlighting the temporal nature of dynamics. (B) In details, group 3 studies the dynamic functional network by examining the nodal connections evolving in time or multiplex networks. (C) Our approach differs from group 3 in that we study the dynamic functional connectivity by the construction of transition networks where each node is a meta-state and the links between nodes are the transitions between meta-states, and analyse the temporal order in meta-states were visited.

3422x1205mm (72 x 72 DPI)

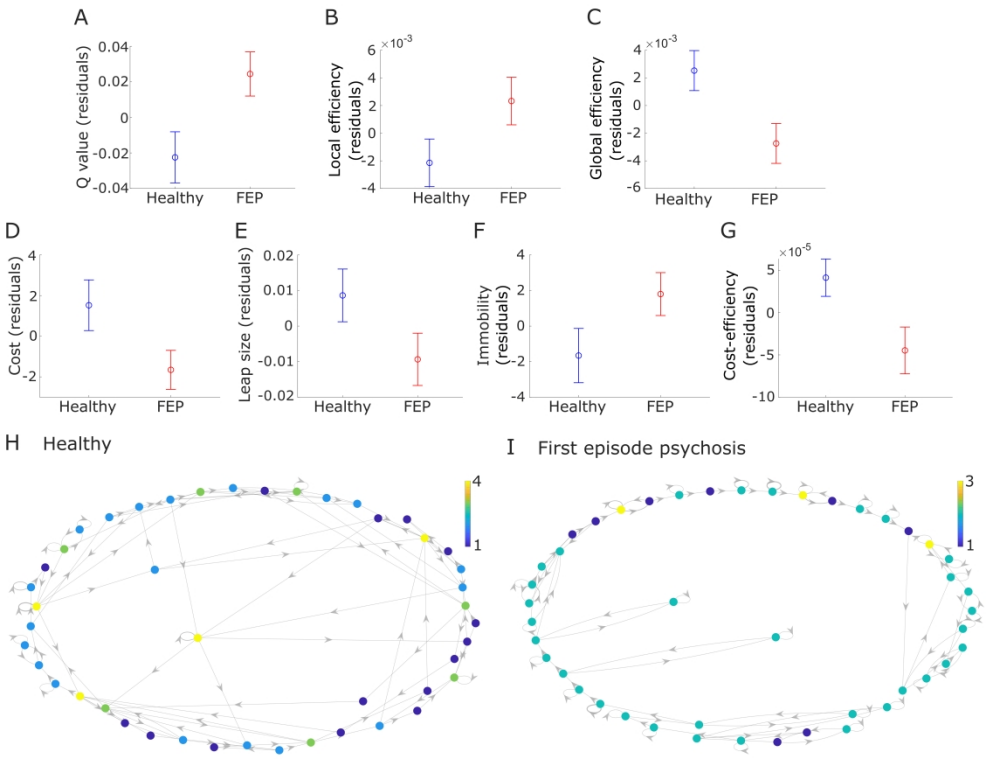

Figure 2. Topological and economical properties of transition networks and transition network examples of patients with first episode psychosis and healthy controls.

The plots show the residuals of the area under the curve for topological and economical properties in the transition graph for healthy controls (blue) and patients with first episode of psychosis (red). A, modularity (Q value). B, local efficiency. C, global efficiency. D, Transition cost. E, Leap size. F, Immobility. G, Cost-efficiency. The circles and error bar mark the mean and standard error of the mean.

The bottom figures shows transition networks from two subjects. Column H shows healthy control and column I, patient. The layout of the graph is such that the distance between nodes is proportional to their transition cost (1 – correlation of connectivity matrices). The color of the nodes denote the degree, the arrow of links represent the direction, and the width of links the number of transitions between the connected nodes (weight). Self-connections of the nodes represent consecutive periods (time windows) in which the brain remained in the same meta-state (i.e. immobility). The temporal path depicted in the transition graph of the healthy control spans longer distances (larger leap size), reaching other nodes rapidly (higher global efficiency), with apparently less redundant paths (lower local efficiency). In the transition network of the patient the nodes are less connected, which implies going through more intermediate nodes to visiting meta-states (lower global efficiency)".

1952x1512mm (72 x 72 DPI)

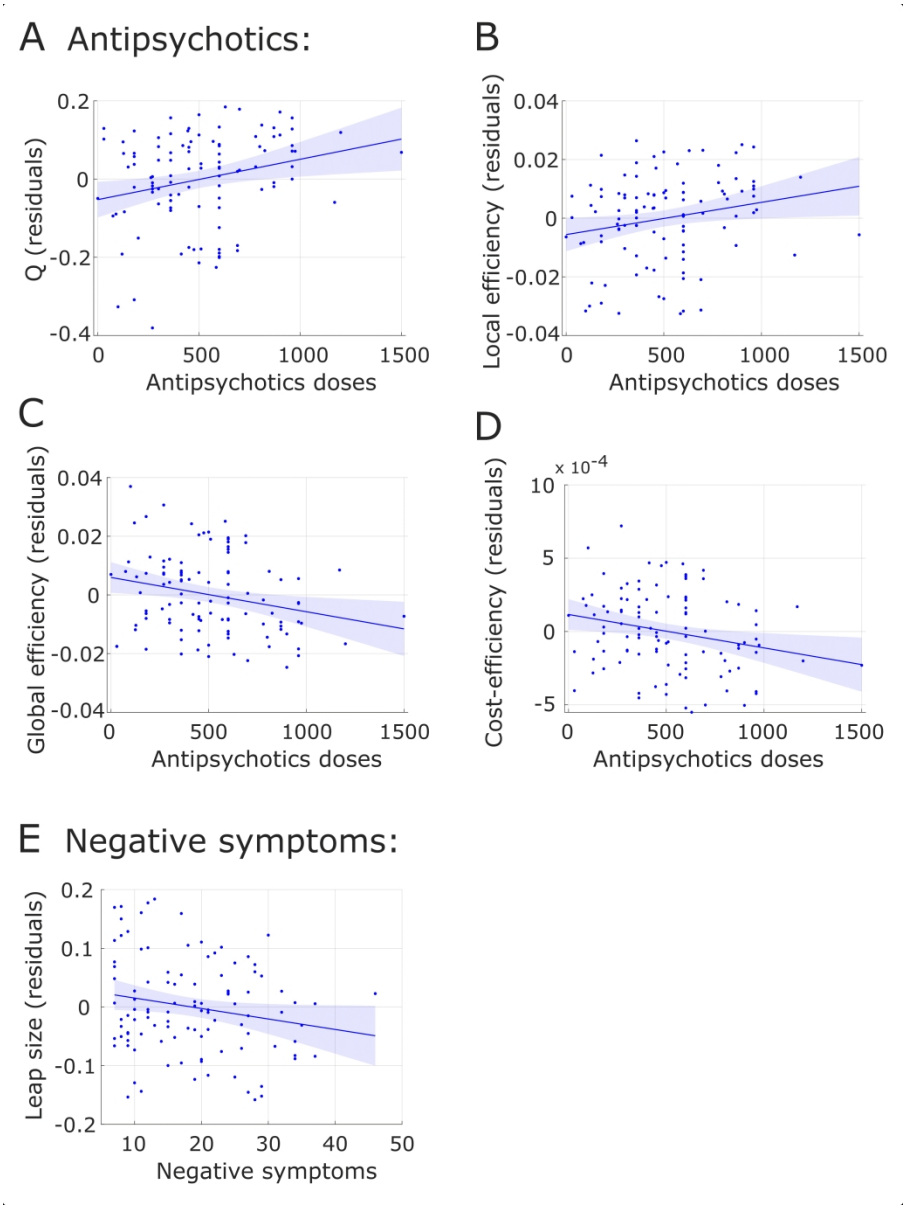

Figure 3. Transition network properties are related to antipsychotic doses and negative symptoms. Scatter plots A-D show significant associations between topological characteristics of the transition networks in patients and antipsychotic doses. A, modularity (Q value). B, local efficiency. C, global efficiency. D, Cost-efficiency. Scatter plot E show significant association between patient's leap size and negative symptoms. The error bar around the linear regression mark 95% CI.

1092x1455mm (72 x 72 DPI)

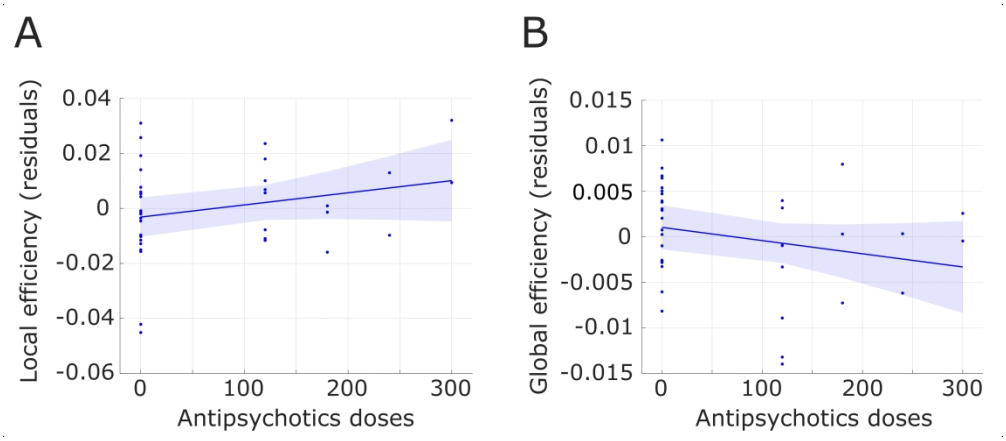

Figure 4. Transition network properties are related to antipsychotic doses in the Mexican sample
Scatter plots showing the significant associations between topological characteristics of the transition networks in patients and antipsychotics doses. A, local efficiency. B, global efficiency. The error bar around the linear regression mark 95% CI.

1674x724mm (72 x 72 DPI)

Supplementary Information for

Dysconnectivity in schizophrenia revisited: abnormal temporal organization of dynamic functional connectivity in patients with a first episode of psychosis

Juan P. Ramirez-Mahaluf, Ángeles Tepper, Luz Maria Alliende, Carlos Mena, Carmen Paz Castañeda, Barbara Iruretagoyena, Ruben Nachar, Francisco Reyes-Madrigal, Pablo León-Ortiz, Ricardo Mora-Durán, Tomas Ossandon, Alfonso Gonzalez-Valderrama, Juan Undurraga, Camilo de la Fuente-Sandoval, Nicolas A. Crossley.

This PDF file includes:

- **Supplementary Figures:**
  - **Figure S1:** Construction of transition networks.
  - **Figure S2:** Directed and undirected graph differences.
  - **Figure S3**: Topological and economical properties of transition networks before and after treatment in patients with complete follow-up of Chilean sample.
  - **Figure S4**: Topological and economical properties of transition networks before and after treatment in patients with complete follow-up of Mexican sample.
  - **Figure S5:** Topological and economical properties of transition networks in Mexican healthy controls
  - **Figure S6:** Reliability of Leap Size
  - **Figure S7:** Topological and economical properties of transition networks in antipsychotics-naïve first episode of psychosis and healthy controls.

- **Supplementary Tables:**
  - **Table S1:** Antipsychotic medications of Chilean and Mexican cohorts
  - **Table S2:** Demographical and clinical scales of Chilean cohort organized according to repeated measures
  - **Table S3:** Demographical and clinical scales of Chilean cohort organized according to repeated measures
  - **Table S4:** Properties of transition networks before and after treatment in patients with complete follow-up of Chilean sample.
  - **Table S5:** Properties of transition networks before and after treatment in patients with complete follow-up of Mexican sample.
  - **Table S6:** Linear mixed-effect model results for the topological and economical properties of transition networks in first episode of psychosis and healthy controls (Chilean sample)
  - **Table S7:** Linear mixed-effect model results for the topological and economical properties of transition networks in first episode of psychosis (Chilean sample)
  - **Table S8:** Reliability of graph metrics
  - **Table S9:** Linear mixed-effect model results for the topological and economical properties of transition networks in antipsychotics-naïve first episode of psychosis patients and healthy controls (Mexican sample)
  - **Table S10:** Linear mixed-effect model results for the topological and economical properties of transition networks in antipsychotics-naïve first episode of psychosis patients (lower doses antipsychotics at follow-up, Mexican sample)

Transition network construction:

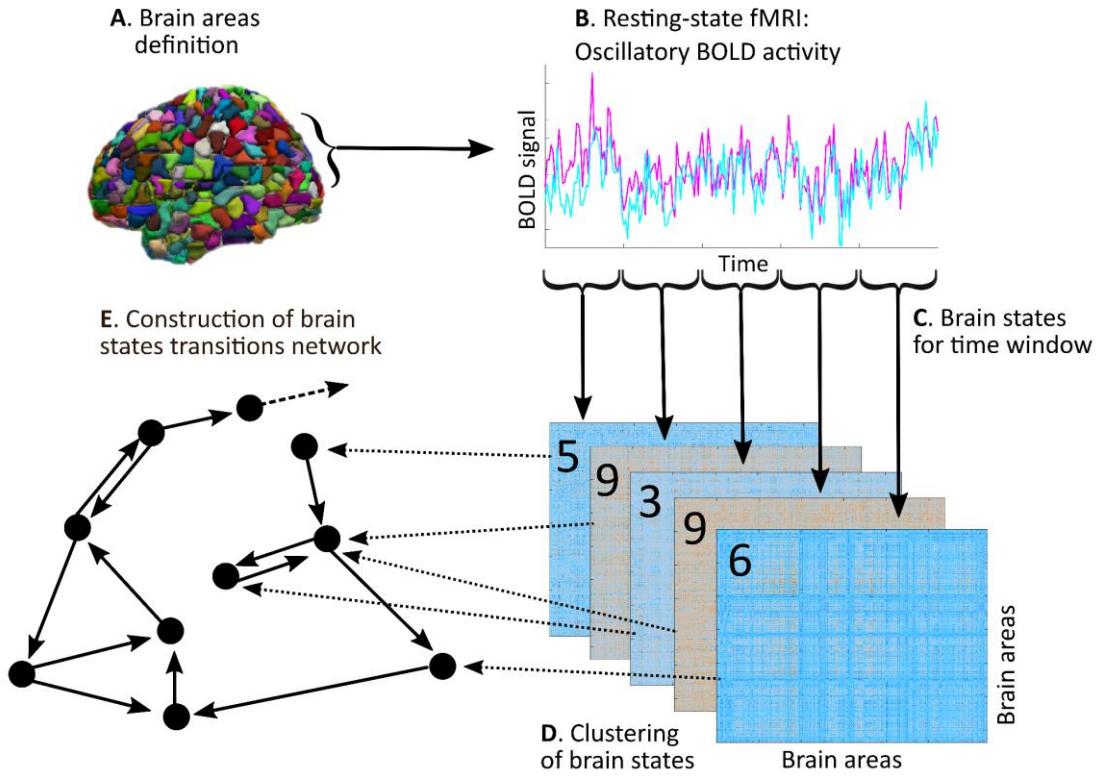

Figure supplementary 1. Construction of transition networks.

Brain areas are defined using a template (A), and their average time course is extracted (B). A measure of functional connectivity, namely multiplication time derivatives, is measured between all pairs of regions for each non-overlapping time window of approximately 5 seconds (2 TRs). Functional connectivity across regions within the window defines a brain state (C), which are clustered to allocate them to specific meta-states (D). Finally, the directed graph of the trajectory taken by the brain through each meta-state is calculated (E). Note that connections between two nodes A to B and B to A in the resulting directed graph are not equivalent.

As described in the main text, we built directed graphs to represent the changing configurations of the functional brain network in time. Links in directed graphs also represent a specific direction, which in our case follows the passage of time. Links in more commonly used undirected graph represent bidirectional connections. This characteristic is particularly relevant for path-length based metrics such as global-efficiency, local efficiency and cost-efficiency. This is shown in figure S2, where blue lines indicate differences in the shortest path reconstructed from similar nodes (in green) in directed and undirected networks. Note that due to the restriction of the direction of the flow, the directed graph has a longer shortest path. Similarly, redundant trajectories in neighbours of a node need to be cyclic to be counted for clustering/local efficiency in directed graphs.

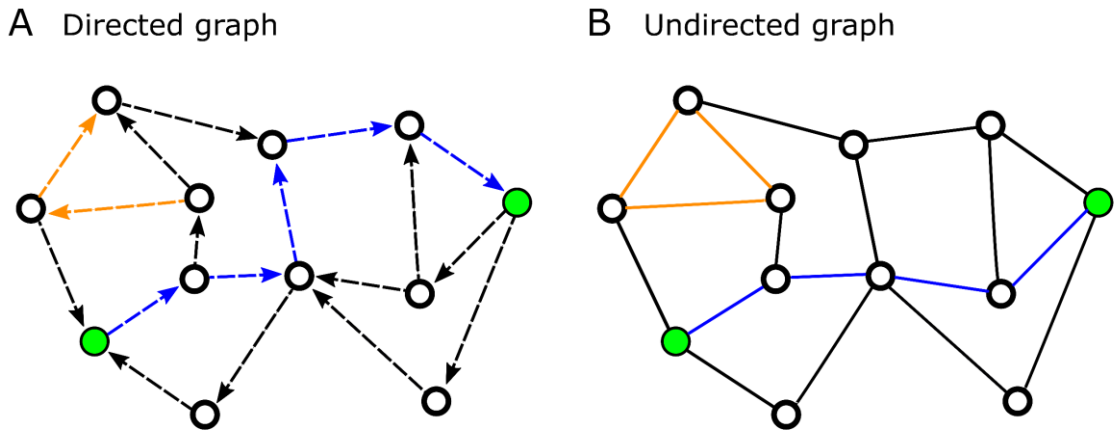

Figure supplementary 2. Directed and undirected graph differences.

(A) Directed graph, (B) Undirected graph. Blue lines indicate path length (global efficiency). Orange lines indicate local efficiency.

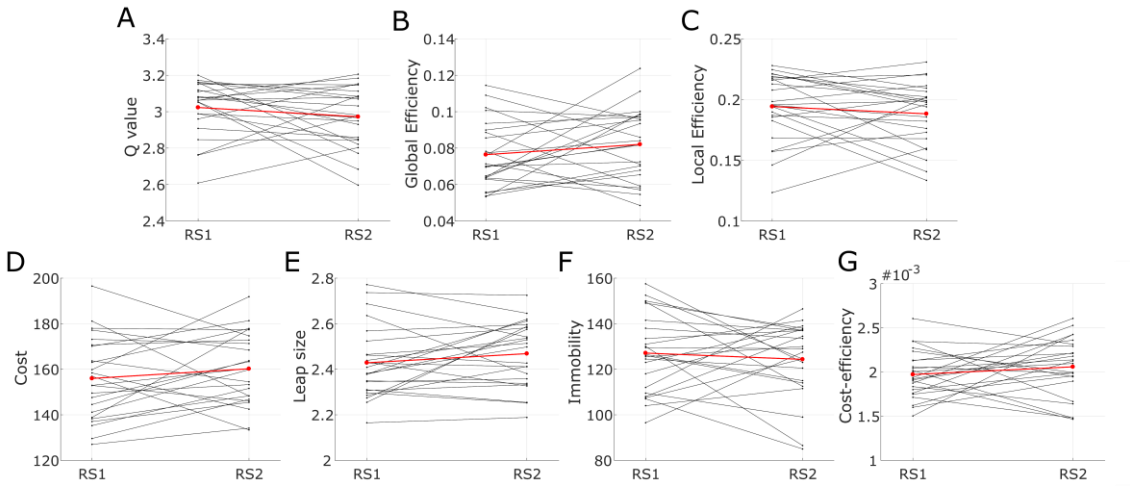

Figure supplementary 3. Topological and economical properties of transition networks before and after treatment in patients with complete follow-up of Chilean sample. A-G plot show the repeated measurements from subjects with two scans. **(A)** modularity (Q value), **(B)** global efficiency, **(C)** local efficiency, **(D)** Transition cost, **(E)** Leap size, **(F)** Immobility and **(E)** Cost-Efficiency. Each subject are plotted in black and the mean are plotted in red. RS1= resting state 1, RS2=resting state 2.

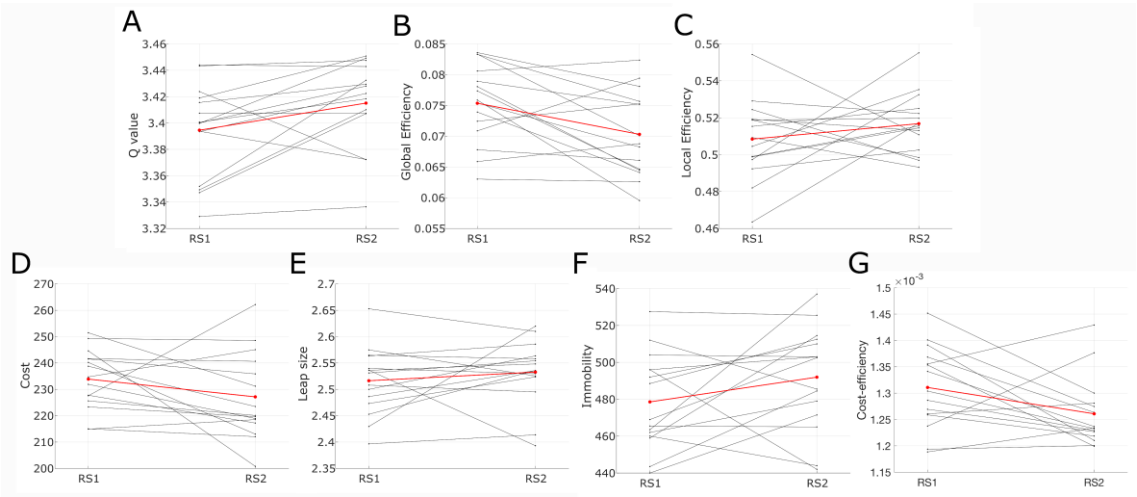

Figure supplementary 4. Topological and economical properties of transition networks before and after treatment in patients with complete follow-up of Mexican sample. A-G plot show the repeated measurements from subjects with two scans. **(A)** modularity (Q value), **(B)** global efficiency, **(C)** local efficiency, **(D)** Transition cost, **(E)** Leap size **(F)**, Immobility and **(E)** Cost-Efficiency. Each subject are plotted in black and the mean are plotted in red. RS1= resting state 1, RS2=resting state 2.

In the following supplementary figures 5 we compared the observed transition-network parameters with 2 different null models: *Random null model,* where the probability of the transition from one meta-state to another one was completely random, generating a random network (100 iterations)[1] and *Degree conserved null model,* where the rewiring of the network was performed in such a way that the distribution of the number of connections to nodes, or the degree distribution of the network, was maintained (100 iterations)[2]. This was accomplished by scrambling the full path of transitions underwent by brain dynamics (for example, from ABABCABCD to AADBACBCB). For details see Ramirez-Mahaluf, et al. 2020[3]. Mexican sample showed a non-trivial temporal organization in their brain dynamics, such as a high clustering, and a modular organization. This organization was implemented at a low biological cost with a high cost-efficiency of the dynamics.

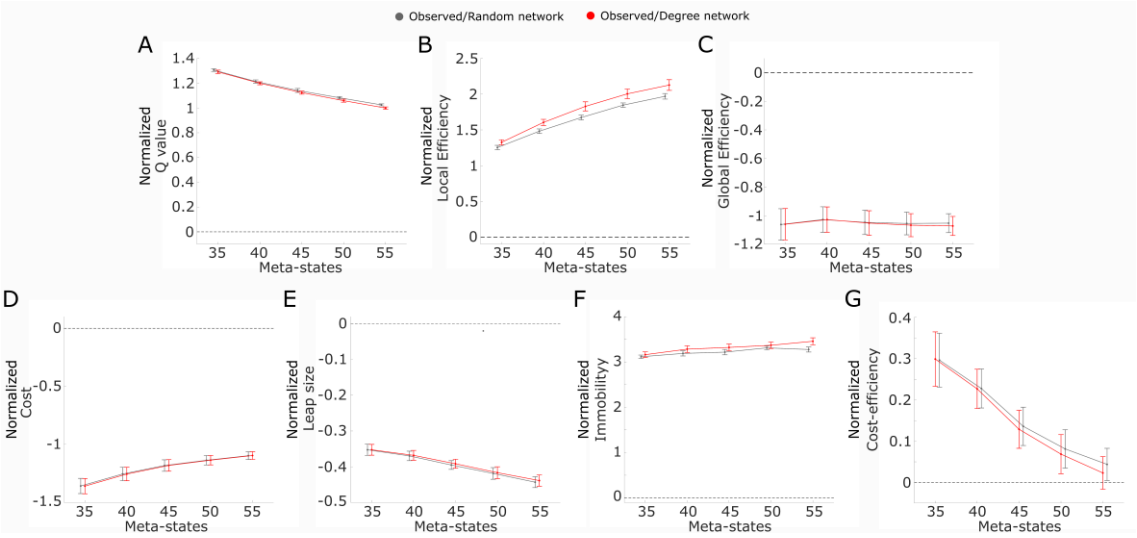

Figure supplementary 5. Topological and economical properties of transition networks in Mexican healthy controls.

A-G describe the ratio between the observed property in the transition graph and different null models for **(A)** modularity (Q value), **(B)** local efficiency, **(C)** global efficiency, **(D)** Transition cost, **(E)** Leap size, **(F)** Immobility and **(E)** Cost-Efficiency. The ratios between the transition network and a null model are plotted alongside its 95% confidence interval of the mean. Dotted lines mark the line of no difference with the null models. Comparisons with random null model networks are plotted in gray, with degree-conserved null network in red.

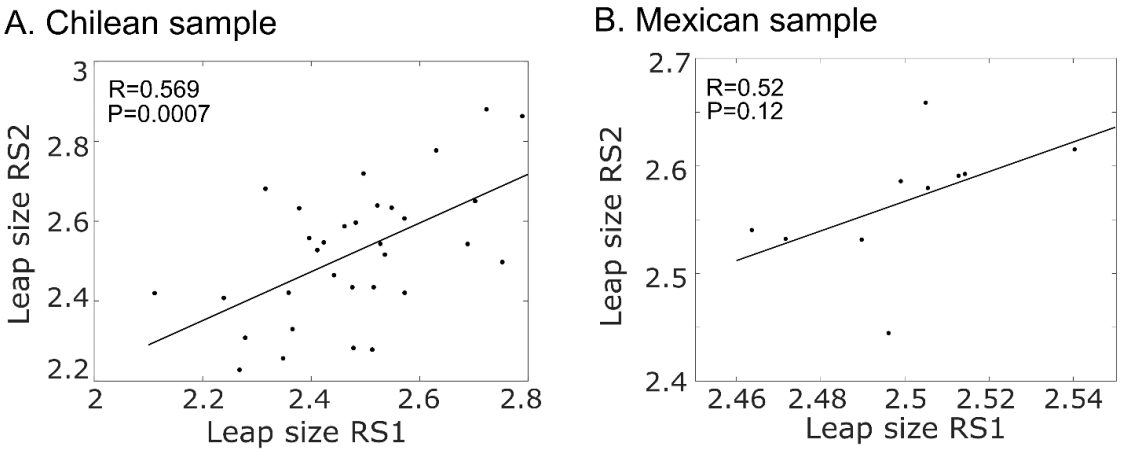

Figure supplementary 6. Reliability of Leap Size.
Scatter plots showing the correlations between Leap size during resting state 1 (RS1) and during resting state 2 (RS2). Chilean sample **(A)** and Mexican Sample **(B)**.

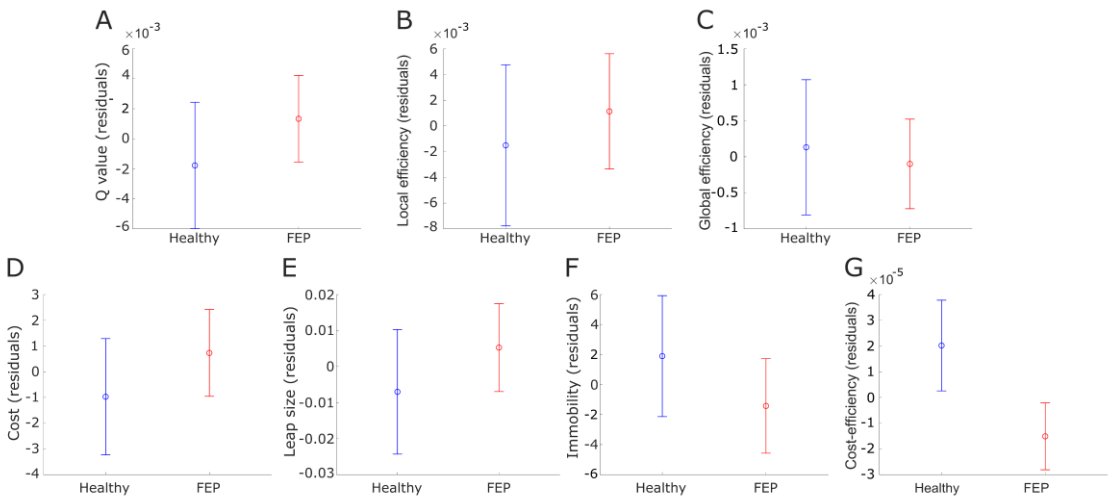

Figure supplementary 7. Topological and economical properties of transition networks in antipsychotics-naïve first episode of psychosis and healthy controls.

The plots show the residuals of the area under the curve for topological and economical properties in the transition graph for healthy controls (blue) and patients with first episode of psychosis (red). **A**, modularity (*Q* value). **B**, local efficiency. **C**, global efficiency. **D**, Transition cost. **E**, Leap size. **F**, Immobility. **G**, Cost-efficiency. The circles and error bar mark the mean and standard error of the mean. FEP= First episode of psychosis.

	Chilean sample		*Mexican sample*	
	Baseline	*Follow-up*	*Baseline*	*Follow-up*
Second generation				
Olanzapine	17.1 ± 5.7 (47)	16.7 ± 3.9 (12)	0 ± 0	0 ± 0
Risperidone	4.5 ± 1.7 (46)	3.2 ± 2.0 (9)	0 ± 0	2.87 ± 0.3 (15)
Aripiprazole	18.5 ± 8.0 (11)	18.1 ± 11.4 (4)	0 ± 0	0 ± 0
Clozapine	116.7 ± 62.9 (3)	250 ± 100 (4)	0 ± 0	0 ± 0
Quetiapine	116.7 ± 57.7 (3)	300 (1)	0 ± 0	0 ± 0
Amisulpride	300 (1)	100 (1)	0 ± 0	0 ± 0
First generation				
Haloperidol	6.8 ± 4.6 (2)	0 ± 0	0 ± 0	0 ± 0
Fluphenazine decanoate	0 ± 0	18mg/ml every 21 days (1)	0 ± 0	0 ± 0

Table supplementary 1. Antipsychotic medications of Chilean and Mexican cohorts. Mean ± standard deviation (N)

	With repeated measures		Without repeated measures	
	First evaluation	Second evaluation	First evaluation	Second evaluation
Demographical variables				
N Baseline (male)	24 (17)	24 (17)	55 (47)	3 (3)
Age	20.6 ± 0.6	20.6 ± 0.6	19.9 ±0.4	18.7 ±0.9
Non-affective psychosis	19	19	48	3
Clinical scales and antipsychotic doses in patients				
	Baseline	*Follow-up*	*Baseline*	*Follow-up*
PANSS total	69.9±3.2	44±3.2	69.1±2.6	48.7±14.2
PANSS Positive symptoms	16.8±1.4	9.6±0.8	16.1±0.7	9±1
PANSS Negative symptoms	20.4±1.8	12.8±1.4	20.4±1.1	16.3±9.3
PANSS General symptoms	32.4±1.4	21.7±1.3	32.7±1.2	23.3±4.4
MATRICS total score	23.5±3.4	33.7±3.3	32.6±2.2	35.7±3.3
Antipsychotic doses (mg)*	527.2±69.3	413 ±52.5	541.8±37.2	590 ±164.6

*Antipsychotic doses expressed in chlorpromazine equivalents (Leucht et al. 2016)

Table supplementary 2. Demographical and clinical scales of Chilean sample organized according to repeated measures.
Mean ± standard error of the mean

	With repeated measures		Without repeated measures	
	First evaluation	Second evaluation	First evaluation	Second evaluation
Demographical variables				
N Baseline (male)	15 (8)	15 (8)	6 (3)	0
Age	26.6 ± 1.8	26.6 ± 1.8	31 ±3.4	
Non-affective psychosis	15	15	6	
Clinical scales and antipsychotic doses in patients				
	Baseline	*Follow-up*	*Baseline*	*Follow-up*
PANSS total	111.3±6.1	75.9±7.5	108.1±7.7	
PANSS Positive symptoms	29.5±1.5	17.3±2.2	30.5±1.8	
PANSS Negative symptoms	27.7±2.7	21.6±2.97	23.8±2.9	
PANSS General symptoms	54.1±2.9	37.1±3.1	53.7±4.2	
MATRICS total score	23.6±3.2	30.3±2.8	27.2±4.9	
Antipsychotic doses (mg)*	0±0	172 ±17.4	0±0	

*Antipsychotic doses expressed in chlorpromazine equivalents (Leucht et al. 2016)

Table supplementary 3. Demographical and clinical scales of Mexican sample organized according to repeated measures.
Mean ± standard error of the mean

Properties	*Resting state 1*	*Resting state 2*	*p-Value*
Modularity	3.023 ± 0.031	2.941 ± 0.034	0.2278
Local efficiency	0.194 ± 0.006	0.187 ± 0.005	0.3249
Global efficiency	0.076 ± 0.004	0.084 ± 0.004	0.2533
Cost	155.96 ± 3.68	163.91 ± 3.121	0.2417
Leap size	2.428 ± 0.032	2.46 ± 0.029	0.1747
Immobility	127.1 ± 3.495	1117.6 ± 3.36	0.5296
Cost-efficiency	0.002 ± 5.4e-05	0.002 ± 6.7e-05	0.3127

Table supplementary 4. Properties of transition networks before and after treatment in patients with complete follow-up of Chilean sample.
Mean ± standard error of the mean. P-values calculated with paired sample t-test.

Properties	*Resting state 1*	*Resting state 2*	*p-Value*
Modularity	3.395 ± 0.009	3.415 ± 0.009	0.0347
Local efficiency	0.508 ± 0.006	0.517 ± 0.004	0.3012
Global efficiency	0.075 ± 0.002	0.070 ± 0.002	0.0182
Cost	233.9 ± 2.943	227.1 ± 4.233	0.1587
Leap size	2.516 ± 0.017	2.533 ± 0.016	0.3989
Immobility	478.6 ± 6.638	492.97 ± 7.23	0.1316
Cost-efficiency	0.001 ± 2.0e-05	0.001 ± 1.7e-05	0.0549

Table supplementary 5. Properties of transition networks before and after treatment in patients with complete follow-up of Mexican sample.

Mean ± standard error of the mean. P-values calculated with paired sample t-test.

Properties	*Estimate*	*SE*	*tStat*	*p-Value*	*p-Value (FDR)*
Modularity	0.041	0.014	2.945	0.004	0.013
Local efficiency	0.005	0.002	2.262	0.025	0.029
Global efficiency	-0.004	0.001	-3.050	0.003	0.013
Cost	-3.761	1.481	-2.539	0.012	0.021
Leap size	-0.028	0.012	-2.314	0.022	0.029
Immobility	3.087	1.453	2.125	0.035	0.035
Cost-efficiency	-5.372e-05	1.949e-05	-2.756	0.006	0.015

Table supplementary 6. Linear mixed-effect model results for the topological and economical properties of transition networks in first episode of psychosis and healthy controls (Chilean sample).

Estimated values of the coefficient (fixed effect variable: patients=1, controls=-1), standard error (SE) of the coefficient, *t*-statistics (tStat) for testing the null hypothesis (coefficient being equal to zero), the *p*-value for the *t*-test and corrected p-value (FDR=false discovery rate). The models also included other variables of no interest (fixed effect): age, gender, frame wise displacement and subjects (random effect).

Properties	*Estimate*	*SE*	*tStat*	*p-Value*	*p-Value (FDR)*
Antipsychotics Doses					
Modularity	0.0002	5.579e-05	3.4034	<0.001	0.021
Global efficiency	-2.042e-05	6.23e-06	-3.276	0.002	0.021
Local efficiency	2.49e-05	9.086e-06	2.7376	0.007	0.041
Cost	-0.0139	0.0055	-2.5135	0.014	0.064
Leap size	-0.0001	5.05e-05	-2.3275	0.022	0.075
Cost-efficiency	-3.023e-07	1.03e-07	-2.9435	0.004	0.038
Negative Symptoms					
Leap Size	-0.0051	0.0018	-2.8432	0.005	0.038
Positive Symptoms					
Leap Size	0.0052	0.0021	2.4474	0.016	0.065

Table supplementary 7. Linear mixed-effect model results for the topological and economical properties of transition networks in first episode of psychosis (Chilean sample).

Estimated values of the coefficient for fixed effect variable: Antipsychotics doses, negative symptoms and positive symptoms, standard error (SE) of the coefficient, *t*-statistics (tStat) for testing the null hypothesis (coefficient being equal to zero), the *p*-value for the *t*-test and corrected p-value (FDR=false discovery rate). The models also included the cognitive symptoms as variable interest (fixed effect), variables of no interest (fixed effect): age, gender, frame wise displacement and subjects (random effect).

Properties	*Correlations*	*p-Value*	*p-Value (FDR)*
Modularity	0.2780	0.1234	0.1440
Local efficiency	0.3110	0.0831	0.3615
Global efficiency	0.1668	0.3615	0.1440
Cost	0.4710	0.0065	0.0228
Leap size	0.5693	0.0007	0.0047
Immobility	0.3014	0.0937	0.1440
Cost-efficiency	-0.2865	0.1119	0.1440

Table supplementary 8. Reliability of graph metrics

Pearson correlation coefficients and p-values between graph measures during resting state 1 and graph measures during resting state 2 in the Chilean sample.

Properties	*Estimate*	*SE*	*tStat*	*p-Value*
Modularity	-0.0002	0.006	-0.032	0.975
Global efficiency	0.0003	0.001	0.232	0.817
Local efficiency	-0.001	0.003	-0.392	0.697
Cost	0.769	1.978	0.389	0.699
Leap size	-0.006	0.008	-0.763	0.449
Immobility	-2.228	3.485	-0.639	0.525
Cost-efficiency	9.471e-07	1.121e-05	0.085	0.933

Table supplementary 9. Linear mixed-effect model results for the topological and economical properties of transition networks in antipsychotics-naïve first episode of psychosis patients and healthy controls (Mexican sample).

Estimated values of the coefficient (fixed effect variable: patients=1, controls=-1), standard error (SE) of the coefficient, *t*-statistics (tStat) for testing the null the null hypothesis that the coefficient is equal to zero, the *p*-value for the *t*-test and corrected p-value (FDR=false discovery rate). The models also included other variables of no interest (fixed effect): age, gender, frame wise displacement and subjects (random effect).

Properties	*Estimate*	*SE*	*tStat*	*p-Value*
Antipsychotics Doses				
Modularity	9.2821e-05	6.4141e-05	1.447	0.159
Local efficiency	7.6259e-05	3.6715e-05	2.077	0.047
Global efficiency	-2.5037e-05	1.2525e-05	-1.999	0.055
Cost	-0.041	0.0266	-1.541	0.135
Leap size	4.6115e-05	0.0001	0.393	0.698
Cost-efficiency	-2.1772e-07	1.318e-07	-1.652	0.109
Negative Symptoms				
Leap Size	0.001	0.0013	0.766	0.450
Positive Symptoms				
Leap Size	-0.0001	0.0015	-0.086	0.932

Table supplementary 10. Linear mixed-effect model results for the topological and economical properties of transition networks in in antipsychotics-naïve first episode of psychosis patients (lower antipsychotic doses at follow-up, Mexican sample)

Estimated values of the coefficient for fixed effect variable: Antipsychotics doses, negative symptoms and positive symptoms, standard error (SE) of the coefficient, *t*-statistics (tStat) for testing the null the null hypothesis that the coefficient is equal to zero, the *p*-value for the *t*-test and corrected p-value (FDR=false discovery rate). The models also included the cognitive symptoms as variable interest (fixed effect), variables of no interest (fixed effect): age, gender, frame wise displacement and subjects (random effect).

References

1. Bullmore E, Sporns O. The economy of brain network organization. *Nat Rev Neurosci*. 2012;13(5):336-349. doi:10.1038/nrn3214
2. Maslov S, Sneppen K. Specificity and stability in topology of protein networks. *Science (80-)*. 2002;296(5569):910-913. doi:10.1126/science.1065103
3. Ramirez-Mahaluf JP, Medel V, Tepper Á, et al. Transitions between human functional brain networks reveal complex, cost-efficient and behaviorally-relevant temporal paths. *Neuroimage*. 2020;219:117027. doi:10.1016/j.neuroimage.2020.117027